Published in final edited form as:
Cancer Res. 2011 June 1; 71(11): 3912–3920. doi:10.1158/0008-5472.CAN-10-2259.

Combining histone deacetylase inhibitor vorinostat with aurora kinase inhibitors enhances lymphoma cell killing with repression of c-Myc, hTERT, and micro-RNA levels

Leo Kretzner[1], **Anna Scuto**[2], **Pamela M. Dino**[5], **Claudia M. Kowolik**[2], **Jun Wu**[1], **Patrick Ventura**[3], **Richard Jove**[2], **Stephen J. Forman**[4], **Yun Yen**[1], and **Mark H. Kirschbaum**[4,5]

[1] Department of Translational Research, Clinical and Molecular Pharmacology, City of Hope and Beckman Research Institute, Duarte, CA, USA

[2] Department of Molecular Medicine, City of Hope and Beckman Research Institute, Duarte, CA, USA

[3] Department of Bio-statistics, City of Hope and Beckman Research Institute, Duarte, CA, USA

[4] Department of Hematology and Hematopoietic Cell Transplantation, City of Hope and Beckman Research Institute, Duarte, CA, USA

[5] Department of Experimental Therapeutics, Nevada Cancer Institute, Las Vegas, NV, USA

Abstract

MK-0457 and MK-5108 are novel aurora kinase inhibitors (AKi) leading to G2/M cell cycle arrest. Growth and survival of multiple lymphoma cell lines were studied with either drug alone or in combination with vorinostat, an HDACi, using MTS and Annexin V assays, followed by molecular studies. Either AKi alone at 100 – 500 nM resulted in ~50% reduced cell growth and 10% – 40% apoptosis. Addition of vorinostat reactivated pro-apoptotic genes and enhanced lymphoma cell death. qPCR and immunoblotting revealed that epigenetic and protein acetylation mechanisms were responsible for this activity. The prosurvival genes Bcl-XL and hTERT were downregulated 5-fold by combination drug treatment, while the proapoptotic Bad and Bid genes were upregulated 3-fold. The p53 tumor suppressor was stabilized by an increased acetylation in response to vorinostat and a reduced Ser315 phosphorylation in response to aurora kinase A. Vorinostat or trichostatin A decreased Myc mRNA and protein as well as Myc-regulated microRNAs. Myc is a critical gene in these responses, as Myc knock-down combined with the expression of the Myc antagonist Mxd1, raised cell sensitivity to the effects of either AKi. Thus, the HDACi vorinostat leads to both transcriptional and post-transcriptional changes to create a pro-apoptotic milieu, sensitizing cells to mitosis-specific agents such as Aki's.

Keywords

Vorinostat; Aurora Kinase; Lymphoma; c-myc; hTERT; miRNA

Corresponding author: Mark H. Kirschbaum, formerly of Department of Hematology/HCT, City of Hope, Duarte, CA. Current contact information: Director, Experimental Therapeutics, Nevada Cancer Institute, Medical Oncology, One Breakthrough Way, Las Vegas NV 89135, Ph: 702.822.5229 Fax: 702.944.1165, mkirschbaum@nvcancer.org.

Conflicts of Interest: Supported in part by a research grant from the Investigator Initiated Studies Program of Merck Sharp & Dohme Corp. The opinions expressed in this paper are those of the authors and do not necessarily represent those of Merck Sharp & Dohme Corp

Introduction

The aurora kinases are Ser/Thr protein kinases active during late G2 and M phases of the cell cycle. Aurora Kinases (AK) A, B, and C regulate key functions during mitosis and thus are logical drug targets for cancer therapies. AK-A is amplified in several tumor types including lymphomas (1), localizes to centrosomes, and is required for spindle body formation. AK-B is present at the midbody of paired sister chromosomes, including the kinetochores. AK-C is expressed predominantly in germ cells and is the least studied member of the family (2). Aurora kinase-A phosphorylates p53 at Ser315, leading to its ubiquitination by MDM2 and subsequent proteolysis (3). Consequently, depleting cells of AK-A with siRNA leads to p53 stabilization and increased numbers of cells in the G2/M cell cycle phase (3). Known AK-B substrates include serine 10 of histone 3 (H3-Ser10) and vimentin (4, 5). Here we test the pan-AK inhibitor MK-0457 (previously VX-680) (2) and the AK-A specific inhibitor, MK-5108, alone and in combination with the deacetylase inhibitor vorinostat.

Agents affecting epigenetic targets, such as histone deacetylase inhibitors (HDACi), may enhance the antitumor activity of antimitotic agents like aurora kinase inhibitors (AKi) in several ways. HDACi's can upregulate genes involved in DNA damage recognition and response, including those directly involved in cell cycle control and apoptosis (6, 7). Furthermore, deacetylase inhibitors can lead to apoptosis through acetylation and stabilization of non-histone proteins such as p53 (8,9). Aurora kinase inhibition primarily leads to cell cycle arrest in the G2/M phase, but not necessarily to cell death. Thus, combining an AKi with an HDACi such as vorinostat (suberoylanilide hydroxamic acid; generic name, vorinostat; trade name, Zolinza®; Merck& Co.) may reactivate the pro-apoptotic capacity of cells and render them more sensitive to apoptosis triggered by cell cycle inhibition. We show this to be the case, and describe changes in gene-expression levels for c-myc, telomerase (hTERT), p53, and microRNAs related to lymphomagenesis (10, 11), which may contribute to the enhanced sensitivity of cells to AKi in the presence of vorinostat.

Materials and Methods

Cell culture and assays

Cells were obtained from ATCC except: L540 cells, from DSMZ; DHL-4 cells, from Dr. Michael Jensen, City of Hope; and KM-H2 cells, from Dr. Markus Müschen, University of Southern California, all of whom verified cell identities. Cells were grown in RPMI-1640 medium plus 10% fetal bovine serum and 50 ng/ml Normocin antibiotic (Amaxa/Lonza Biotechnology, Walkersville, MD). Vorinostat, MK-0457 and MK-5108 were from Merck Inc., and were dissolved in DMSO.

Cell Growth & Survival

MTS assays employed Promega reagents (Madison, WI), according to the manufacturer's protocol. Cells were plated at 5000 cells/well in triplicate wells of 96-well plates and cultured with the drugs indicated in Figure 1 for 72 hours. MTS reagent [3-(4,5-dimethylthiazol-2-yl)-5-(3-carboxymethoxyphenyl)-2-(4-sulfophenyl)-2H-tetrazolium] was added and light readings at 490 nm were taken one to two hours later. Raw values were averaged, background absorbencies (medium without cells) subtracted, and resulting values normalized with control cells grown in 0.1% DMSO set to 1x (100%) growth.

Cell Cycle and Apoptosis assays

Log-phase cells were brought to 0.25×10^6/ml and 1 ml aliquots were plated in 12-well plates with drug concentrations as indicated in figures. After two- and three-day incubations, cells were centrifuged with cold PBS washes. For cell cycle analysis, cells were fixed in 70% ethanol and treated with propidium iodide (PI) staining solution: PBS + 0.1 % (vol/vol) Triton X-100, 0.2 mg/ml RNase A (DNase-free), and 0.02 mg/ml PI. Cells were incubated 15′ at 37° and then overnight at 4° with flow cytometric analysis the next day. For apoptosis determination, cells were assayed using BD Biosciences' (San Jose, CA) Annexin V-FITC Apoptosis Detection Kit 1 according to manufacturer's instructions and analyzed by flow cytometry.

RNA isolation, RT, and qPCR

Cells were washed two times in cold PBS and cell pellets frozen at −80°. For mRNA analysis, RNA was extracted with Qiagen EZ-1 reagents (Valencia, CA) according to manufacturer's recommendations, quantified, and reverse transcribed with Invitrogen (Carlsbad, CA) SuperScript III reagents, with 2 μg total RNA +5 ng/μl random hexamers. One-tenth volumes of RT reactions were analyzed by real-time PCR using Applied Biosystems reagents (ABI; Foster City, CA) using either SYBR-Green or Taq-Man 2x Master Mixes. Reactions were run for 40 cycles of 95° and 60° alternation, for 15 and 30 seconds, respectively. Quantification was relative to multiple housekeeping genes expressed in lymphatic cells, by the geometric-mean method (12).

For miRNA analysis, cell pellets were extracted with *mir*Vana isolation reagents by Ambion (Austin, TX), quantified, and reverse transcribed with miRNA-specific primers and enzyme mix (Ambion or ABI), according to manufacturer's directions. One-tenth volume of RT product was analyzed with separate, miRNA-specific PCR primer pairs (Ambion/ABI). PCR was with ABI reagents, as above, using the ABI 2x SYBR-Green Master Mix with Ambion primers, and ABI 2x TaqMan Universal PCR Master Mix/No AmpErase-UNG reagents with ABI primers. miRNAs were normalized to miRNA-191 (13) and/or the U6 small nuclear RNA.

Immunoblotting

Western blots were performed as described (6). 40 μg of total protein was loaded per lane. All antibodies were from Cell Signaling Technology (Beverly, MA) other than hTERT antibody, from Abcam (Cambridge, UK).

G2/M cell cycle enrichment

Log-phase L540 cells at ~ 0.6×10^6/ml were diluted to 0.25×10^6/ml, grown overnight (~20 hours), and again brought to 0.25×10^6/ml. Cells were divided into four fractions and drugs added as shown in Figure 4B. Cells were incubated for 24 hours, quickly harvested by 4°C centrifugation, washed once with ~500 ml ice-cold PBS, and once with 10 ml of cold-PBS plus protease- and phosphatase inhibitors (Sigma; St Louis, MO). The resulting pellets were lysed and prepared for immunoblotting (6).

Myc knock-down and Mxd1 overexpression

siRNAs directed against c-myc message were sense:
5′CUGAGACAGAUCAGCAACAACCGdAdA3′ and antisense:
5′UUCGGUUGUUGCUGAUCUGUCUCAGGA3′

All nucleotides are ribose form except two at the 3′ end of the sense strand, underlined above. The negative siRNA was the control, #6201, from Cell Signaling Technology

(Beverly, MA). Overexpression of Myc antagonist Mxd1 was from plasmid pRc/CMV (14, designated 'RCMV-Mad') with empty pRc/CMV as control. siRNA-Myc and/or pRc/CMV-Mxd1, or their controls, were introduced into L540 cells by nucleofection using reagents and electroporation device by Amaxa/Lonza (Walkersville, MD). Two million cells, concentrated by centrifugation from log-phase cultures, were used per transfection. Electroporation volume was 100 μl L-buffer mixed with supplement and nucleic acids according to the manufacturer's instructions, using the X-001 electroporation setting. Final concentration of siRNA during electroporation was 400 nM and amount of plasmid per transfection was 2 μg. Five minutes after electroporation, cells were washed out of cuvettes with prewarmed 0.5 ml antibiotic-free RPMI-1640 with 10% fetal bovine serum, and added to an additional one ml of the same medium. The volume was increased by five mls of the same medium the next day. The numbers of viable cells – determined by Trypan-blue exclusion and typically being 70% – 75% – were counted and used at 10,000 live cells per well in 96-well plates for MTS experiments, with drug additions begun the day after transfection. Each drug condition was tested in triplicate wells, and MTS reagent added 72 hours after drug addition (96 hours after transfection).

Statistical Methods

Pairwise comparisons using Dunnett's test were performed to compare apoptosis and cell growth/survival between each drug treatment compared to vorinostat (Figure 1). To evaluate the dose-response relationship of vorinostat to lymphoma cell gene expression, a linear regression was performed for each gene with dose as the independent variable and individual gene expression as the dependent variable (Figure 3). T-tests were conducted to compare micro-RNA expression response between the various vorinostat and AKi treatments compared to the DMSO reference (Figure 5). All significance testing was performed using SAS V9.2 and all reported p-values are two-sided using an alpha level of 0.05.

Results

Vorinostat and Aurora Kinase inhibitors curb lymphoma growth singly and together

We tested single and combined titrations of MK-0457 or MK-5108 and vorinostat in both cell growth and apoptosis assays with Hodgkin lymphoma (HL) cell lines L540 and KM-H2 and with non-Hodgkin lymphoma (NHL) cell lines including Daudi, DHL-4 and DHL-6. Figure 1A shows L540 growth inhibition by each drug, as determined by MTS assays. Inhibition was dose-dependent and combinations of both drugs inhibited cell growth more than any drug alone at the lower doses. We obtained similar results with the other cell lines tested (Table 1 and Supplementary. Figure 1A). Order-of-addition experiments showed no greater effect than with simultaneous addition of drugs (data not shown).

These data allowed us to calculate IC_{50} and Combination Index (CI) values. Table 1 shows that for most lymphoma cell lines the IC_{50}s of these drugs were in the sub-micromolar range (left half of table). The few exceptions were in relative sensitivities to one or the other AKi. For five of six lines tested – excepting the DHL-6 cells – the IC50's of MK-0457 were lower than those of MK-5108. We also determined Combination Index (CI) values (Table 1, right), showing that combining AKi's MK-0457 or MK-5108 with vorinostat had an additive (CI = 0.85 – 1.1) or frequently synergistic effect (CI = 0.1 – 0.85). There were no consistent differences in CI values between Aki's when combined with vorinostat.

Apoptosis data (Figure 1B) suggested the growth inhibition seen in MTS assays was not primarily due to cell cycle arrest or longer cycling times, but to time- and dose-dependent increases in apoptosis, as assayed by Annexin-V cell labeling. The combination of

vorinostat and an AKi was consistently more effective in promoting cell death than any drug alone in L540 cells, with similar data obtained in Daudi (Supplementary. Figure 1B), KM-H2 and DHL-4 cells (not shown).

The extent of apoptosis with vorinostat plus either AKi was from 2- to 7-fold greater than with either AKi alone, presumably because AK inhibition leads primarily to cell cycle arrest rather than cell death. To discriminate between cell cycle arrest and death, we performed cell cycle analysis, with representative results for L540 cells shown in Figure 2. Incubation in 1.5 μM vorinostat (Fig. 2B) enlarges a modest subpopulation of cells in the sub-G1 region, often indicative of dead cells, while treatment with 100 nM MK-0457 (Fig. 2C) produces a large increase in cells arrested in the G2/M phase, as well as a small increase in the sub-G1 region. Significantly, the two drugs combined shift a substantial proportion of the L540 cells into the sub-G1 population (Fig. 2D). Percentages of cell populations in each cell cycle phase for various treatments are listed in Supplementary Table 1. We obtained similar results with the HL cell line KM-H2 and the NHL cell line Daudi, a Burkitt's lymphoma (Supplementary Figure 2, Supplementary Table 1). The additivity, or in some cases, synergy of these two drugs is reflected in the enrichment of sub-G1 phase cells when both drugs are present. Cell size determination showed most cells treated with MK-0457 were enlarged, whereas those treated additionally with vorinostat were smaller than control cells (not shown), consistent with sub-G1 phase dead and/or dying cells. Along with enlargement, there was evidence of endoreduplication (8N DNA) in some assays, with small cell populations beyond the G2/M peak (not shown). The percentage of apoptosis in each condition exceeds that of cells in sub-G1, as Annexin-V labels intact cells early in apoptosis as well as further degraded ones.

Vorinostat brings about changes in lymphoma cell gene expression

We performed real-time PCR analysis of drug-treated L540 cells to determine reasons for the drugs' effects on the cell cycle and apoptosis. AKi treatment had little effect on expression of the genes we analyzed, in contrast to strong effects seen with HDAC inhibition. Vorinostat led to downregulation of several genes, most notably c-myc (Figure 3A), hTERT and Bcl-X_L (Figure 3B). Vorinostat downregulated another anti-apoptotic gene, Mcl-1, while Bcl-2 levels changed very little (not shown). Since vorinostat downregulated message levels of c-myc, we assayed levels of the Myc-antagonist, Mxd1 (originally Mad1; 14), and found it was simultaneously upregulated (Figure 3A). Such inverse patterns of expression of Myc and Mxd genes have been seen in multiple cell types studied, often in cells exiting the cell cycle and/or undergoing differentiation (15, 16).

In contrast to downregulation of anti-apoptotic Bcl-X_L and Mcl-1, vorinostat upregulated the proapoptotic genes Bad, Bid and Noxa (Figure 3C). Most gene expression changes were apparent within four hours of vorinostat addition (Figures 3A and 3C) and were still variably present at 24 hours for Myc and Mxd1 (Supplementary Figure 2A), hTERT and Bcl-X_L (Figure 3B) and Noxa (Supplementary Figure 2C). However Bad and Bid message level increases were an early event, seen only at the 4 hour time point (Figure 3C). By 24 hours their expression levels were at baseline or somewhat repressed (Supplementary Figure 2C).

Immunoblotting experiments confirmed qPCR results and assessed post-translational changes in L540 cell proteins (Figure 4). Figure 4A, top frame, shows vorinostat concentration-dependent increases in acetylation at the histone H3 lysine-nine residue (H3-K9), which were unchanged by addition of MK-0457. Acetylation of p53 seemed less sensitive to vorinostat than was H3-K9, becoming apparent only at higher concentrations. Acetylation of p53 was also seen in response to MK-0457, with greater response when combined with 3 μM vorinostat (Figure 4A); acetylation of p53 is known to lead to stabilization (17). MK-0457-mediated increased p53 acetylation was associated with

increased protein levels of p53-target $p21^{Waf1/Cip1}$, as well as the mRNA levels of p53-target Noxa (Figure 3C). While the amount of p21 and p27 proteins increased in response to vorinostat or MK-0457 alone and in response to MK-0457 in combination with the lowest dose of vorinostat, the levels of these proteins subsequently decreased in response to MK-0457 in combination with the highest dose of vorinostat. This is in agreement with other studies showing that downregulation of p21 or p27 makes cells more prone to apoptosis (6, 18) and is also consistent with accumulation of cells in sub-G1 (Figure 2). The Western blot data in Figure 4A confirmed at the protein level the downregulation of c-myc and FOXO3A genes detected by qPCR (Figure 3A and not shown). Similarly, Bcl-X_L and Mcl-1 protein levels were also reduced (Figure 4A, bottom panels).

Cell cycle block experiments using the microtubule poison nocodazole allowed us to enrich for protein isoforms transiently present during the G2/M phase that are difficult to detect in nonsynchronized cells (Figure 4B). Utilizing synchronized cell populations we were able to visualize the phosphorylated forms of three aurora kinase targets by Western blot assay. p53 is normally phosphorylated at Ser315 by AK-A, leading to its association with the ubiquitin ligase MDM2 and proteosome destruction (3). Phosphorylation of p53at Ser46 is strongly associated with pro-apoptotic activity of this tumor suppressor (19). Histone H3 is a known substrate for AK-B phosphorylation at Serine 10 resulting in dissociation of heterochromatin protein 1 (HP1) during mitosis. (4). To assess the effects of Aurora Kinase treatment on these substrates, we treated L540 cells with nocodazole, with or without MK-0457, and compared them to cells treated with MK-0457 alone and to control cycling cells. Cell cycle analyses (not shown) indicated MK-0457 and nocodazole both blocked cycling; the nocodazole-treated +/− MK-0457, were similarly enriched for G2/M phase cells (nocodazole, 42%; MK-0457, 45%; both drugs, 53%). All drug-treated cells also had similar viability (nocodazole, 73%; MK-0457, 75%; both drugs, 79%) All three phospho-proteins analyzed were expressed at low levels in cycling cells (Figure 4B, lane 1) but accumulated at detectable levels in the presence of nocodazole. MK-0457 inhibited the phosphorylation of histone H3 in the presence of nocodazole. p53 phosphorylation at both Ser 315 and Ser46, was also inhibited by MK-0457 in the presence of nocodazole.

Vorinostat and AKi treatments lead to changes in micro-RNA levels

Micro-RNAs (miRNAs) are key regulators of cell growth and differentiation by virtue of post-transcriptional inhibition of mRNA stability and/or translation (20, 21). Myc transcriptionally activates the miRNA 17–92 cluster (10, 11). Since vorinostat repressed c-myc message and protein (Figures 3 and 4), we tested expression levels of three members of this miRNA cluster; miR-17.5p, miR-17.3p, and miR-18; in response to vorinostat, the unrelated HDACi trichostatin A (TSA), and MK-0457 in L540 (Figure 5A) and DHL-4 cells (Supplementary Figure 5A). Treatment with HDACi resulted in decreases in all three miRNAs relative to untreated cells HDACi also induced changes in three miRNAs that are not myc-regulated; miR-15b, miR-34a, and miR-155; as shown in Figures 5B and Supplemenary Figure 5B for L540 and DHL-4 cells, respectively. The two cell types have distinct changes in the expression of these miRNAs, possibly reflecting biological differences between the different lymphoma types involved (Hodgkin lymphoma versus B-cell lymphoma).

Role of Myc downregulation and Mxd1 upregulation by vorinostat Aki combination

Lastly, we sought to determine the importance of HDACi-induced c-myc downregulation in lymphoma cell responses to combined HDAC/AK inhibition. To model this downregulation in the absence of HDACi, we transfected L540 cells with small interfering RNA (siRNA) directed at c-myc mRNA, and/or over-expressed the Myc antagonist, Mxd1, followed by titration of either MK-0457 or MK-5108 (Figures 5C and 5D). Knock-down of c-myc

message was difficult in L540 cells, typically reaching a 50% decrease at 48 – 72 hours (not shown). Thus, siRNA-myc had only a small negative effect on cell survival in response to MK-0457 (Figure 5C) and a slightly greater effect with MK-5108 (Figure 5D). Mxd1 over-expression (turquoise line, Figures 5C and 5D) led to similar results. However, upon combining myc knock-down with Mxd1 expression (green lines) L540 cells clearly became more sensitive to both AKi's. The IC_{50} of MK-0457 (blue line, Figure 5C) was lowered from ~0.5 μM to 0.1 μM by combined treatment, while that of MK-5108 (blue line, Figure 5D) went from ~1.8 μM (by extrapolation) to ~0.35 μM. Thus, combining myc knock-down with Mxd1 over-expression recapitulates the synergistic effect of combining vorinostat with the AKi's, which we postulate is due in part to decreased myc levels after treatment.

Discussion

We have studied the effects of MK-0457 and MK-5108, prototype aurora kinase inhibitors, in combination with histone deacetylase inhibitor vorinostat. Both drugs inhibit AK-A andMK-0457 also inhibits AK-B; alone their Aki activity exerts strong negative cell cycle effects on both HL and NHL cells, but has modest consequences for overall cell growth and survival (Figures 1 and 2). We hypothesized that AKi-induced arrest of cells in G2/M phase results in activated intracellular stress signaling pathways, but that in cancer cells this cellular response is blunted by epigenetic silencing of tumor suppressor and pro-apoptotic genes. Thus, the HDACi vorinostat could potentially exert a synergistic or at least additive effect when combined with AKi's. This proves to be the case in lymphoma cells, as also seen in acute and chronic myelogenous leukemia cells when combining vorinostat and MK-0457 (22, 23). Given the similar responses of cells treated with both MK-0457 and MK-5108, we hypothesize that it is inhibition of aurora kinase A that is central to the activity in lymphoma cell lines.

The effects of aurora kinase inhibition on gene expression levels are modest, while those of vorinostat are extensive. Key effects of HDAC inhibition were downregulation of c-Myc, hTERT, Bcl-X_L, Mcl-1 and FoxO3A, and upregulation of cell cycle inhibitors p21 and p27 and the pro-apoptotic genes Bad, Bid, and Noxa, seen in both qPCR and immunoblot assays. Immunoblotting also demonstrated post-translational effects of vorinostat and MK-0457 on p53, leading to stabilization and increased activity of p53.

Telomerase expression often plays a critical role in cancer cell progression, including hematologic neoplasias (24). The rate-limiting component of the telomerase holoenzyme is the catalytic subunit, human telomerase enzymatic reverse transcriptase, hTERT (25). HDACi-induced hTERT regulation has been seen in many cell types (26, 27), typcially in the form of hTERT derepression (28, 29). This report is the first describing hTERT downregulation, with a 25-fold decrease in gene expression following HDAC inhibition in lymphoma cells The mechanistic reasons for this unique result are unclear and may have interesting cell-type specific implications. The hTERT gene is a positive transcriptional target of Myc and is repressed by the Mxd proteins (30, 31). Vorinostat-induced Myc downregulation and Mxd1 upregulation in lymphoma cells can thus explain hTERT gene repression. Increased telomerase expression can accompany disease progression, *e.g.*, higher expression in chronic myelogenous leukemia (CML) blast crisis patients compared to those in the chronic phase (32). Notably, successful imatinib mesylate treatment of CML reduces telomerase activity (33), while high telomerase levels correlate with imatinib resistance (34). These observations suggest HDACi-induced hTERT downregulation is a biologically significant event in vorinostat inhibition of lymphoma cell growth.

MicroRNAs are key regulators of cell growth and differentiation due to messenger RNA downregulation (20, 21). Their differential expression can be used to classify multiple

human tumor types, including subtypes of lymphomas (35, 36). We show dose-dependent downregulation of miR-17-5p, miR-17-3p, and miR-18 by vorinostat and TSA in L540 and DHL4 cells. These miRNAs are part of the miR-17-92 miRNA cluster, which is myc-regulated and oncogenic in a Burkitt lymphoma mouse model, and is also implicated in other cancers (10. 11, 37). HDACi downregulation of these miRNAs is thus biologically significant and mechanistically plausible, given simultaneous repression of myc levels by HDACi.

Three other non-myc-regulated miRNAs of significance in lymphomas and other hematologic cancers, miR-15b, miR-34a, and miR-155 exhibited responses to HDAC inhibition. MicroRNAs of the miR-15 and miR-16 family target the mRNA of Bcl-2 and their upregulation is thus associated with apoptosis (38, 39). We saw dose-dependent downregulation of miR-15b in L540 and DHL-4 cell lines by vorinostat or TSA. miR-34a is a positive transcriptional target of p53 (40) and was strongly upregulated in DHL-4 cells (Suplementary Figure 5); however, its levels declined in L540 cells with HDACi treatment (Figure 5). miR-155 is generated from sequences within the non-protein-coding BIC RNA, and both RNAs are upregulated in some HL and DLBCL samples correlating with the activated B cell phenotype (41, 42). miR-155 also has anti-proliferative and pro-apoptotic activities in melanoma cells and hematopoietic stem cells (43, 44). We observed increases in miR-155 after HDACi treatment in L540 cells, although it was repressed in DHL-4 cells. Variable behavior of miR-34a and miR-155 may reflect the different lymphoma types represented by L540 and DHL-4 cells. Differential effects on cells, of changes in the microRNA levels after treatment, as opposed to steady state overexpression, may contribute to differences in miR-155 activity between cell types.

We have demonstrated the importance of myc downregulation in response to vorinostat alone and in the combined response to AKI's and HDACi's. In another hematopoietic malignancy model, reduced myc levels are critical for acute myeloid leukemia cell growth arrest by the HDACi valproic acid (45). Myc levels decline in many cell types undergoing differentiation, while those of Mxd genes rise (15, 16). This counterbalance is consistent with a requirement for both Myc knockdown and Mxd1 over-expression combined with Aki treatment, to mimic the synergistic effect of vorinostat combined with an AKi. Deacetylase inhibitors are under intense study in hematologic malignancies, with vorinostat currently FDA-approved for treatment of cutaneous T cell lymphoma (46). HDAC inhibitory agents have multiple activities in lymphoid cells, ranging from direct antitumor activity to suppression of the activated immune response and cytokine storm (47). We have demonstrated the effects of vorinostat on various targets, such as p53, hTERT, bcl-2 family members, c-myc, and multiple microRNAs. This data strengthens the hypothesis that treatment of tumor cells with deacetylase inhibitors promotes a set of pro-apoptotic changes at the epigenetic and protein level. This is consistent with data reported in various leukemia types treated with vorinostat (22, 23), in which changes in pro-apoptotic protein levels led to enhanced activity when combined with aurora kinase inhibitors. Elucidating the mechanisms by which HDACi's sensitize lymphoma cells to other agents should assist in the development of clinical combination trials. Our data suggest one such trial should include the combination of deacetylase inhibitors with mitotic deregulators such as aurora kinase inhibitors.

Supplementary Material

Refer to Web version on PubMed Central for supplementary material.

Acknowledgments

We greatly thank Sandra Thomas for assembling the final figures and editing the manuscript. This work was supported by the following grants and awards: NIH P50 CA107399, The Tim Nesvig Lymphoma Research Fund, a W.M. Keck Foundation Fellowship to Anna Scuto, and a research award to Dr. Kirschbaum from Merck.

This work was supported by the following grants and awards: NIH P50 CA107399, The Tim Nesvig Lymphoma Research Fund (MK and AS), the W.M. Keck Foundation (AS) and a research award from Merck (MK).

References

1. Yakyshijin Y, Hamada M, Yasukawa M. The expression of the Aurora-A gene and its significance with tumorigenesis in non-Hodgkin's lymphoma. Leuk Lymph. 2004; 45:1741–6.
2. Harrington EA, Bebbington D, Moore J, et al. VX-680, a potent and selective small-molecule inhibitor of the Aurora kinases, suppresses tumor growth in vivo. Nat Med. 2004; 10:262–7. [PubMed: 14981513]
3. Katayama H, Sasai K, Kawai H, et al. Phosphorylation by aurora kinase A induces Mdm2-mediated destabilization and inhibition of p53. Nat Genet. 2004; 36:55–62. [PubMed: 14702041]
4. Hirota T, Lipp JJ, Toh BH, Peters JM. Histone H3 serine 10 phosphorylation by Aurora B cause HP1 dissociation from heterochromatin. Nature. 2005; 438:1176–80. [PubMed: 16222244]
5. Goto H, Yasui Y, Kawajiri A, et al. Aurora-B regulates the cleavage furrow-specific vimentin phosphorylation in the cytokinetic process. J Biol Chem. 2003; 278:8526–30. [PubMed: 12458200]
6. Scuto A, Kirschbaum M, Kowolik C, et al. The novel histone deacetylase inhibitor, LBH589, induces expression of DNA damage response genes and apoptosis in Ph- acute lymphoblastic leukemia cells. Blood. 2008; 111:5093–100. [PubMed: 18349321]
7. Buglio D, Georgakis GV, Hanabuchi S, et al. Vorinostat inhibits STAT6-mediated T_H2 cytokine and TARC production and induces cell death in Hodgkin lymphoma cell lines. Blood. 2008; 112:1424–33. [PubMed: 18541724]
8. Henderson C, Mizzau M, Paroni G, Maestro R, Schneider C, Brancolini C. Role of caspases, Bid, and p53 in the apoptotic response triggered by histone deacetylase inhibitors trichostatin-A (TSA) and suberoylanilide hydroxamic acid (SAHA). J Biol Chem. 2003; 278:1257–89.
9. Johnstone RW, Licht JD. Histone deacetylase inhibitors in cancer therapy: Is transcription the primary target? Cancer Cell. 2003; 4:13–8. [PubMed: 12892709]
10. He L, Thomson JM, Hemann MT, et al. A microRNA polycistron as a potential human oncogene. Nature. 2005; 435:828–33. [PubMed: 15944707]
11. O'Donnell KA, Wentzel EA, Zeller KI, Dang CF, Mendell JT. c-Myc-regulated microRNAs modulate E2F1 expression. Nature. 2005; 435:839–43. [PubMed: 15944709]
12. Vandesompele J, DePreter K, Pattyn F, et al. Accurate normalization of real-time quantitative RT-PCR data by geometric averaging of multiple internal control genes. Genome Biol. 2002; 3:1–12.
13. Peltier HJ, Latham GJ. Normalization of microRNA expression levels in quantitative RT-PCR assays: identification of suitable reference RNA targets in normal and cancerous human solid tissues. RNA. 2008; 14:844–52. [PubMed: 18375788]
14. Ayer DE, Kretzner L, Eisenman RN. Mad: A heterodimeric partner for Max that antagonizes Myc transcriptional activity. Cell. 1993; 72:211–22. [PubMed: 8425218]
15. Rottmann S, Lüscher B. The Mad side of the Max network: antagonizing the function of Myc and more. Curr Top Microbiol Immunol. 2006; 302:63–122. [PubMed: 16620026]
16. Xu D, Popov N, Hou M, et al. Switch from Myc/Max to Mad1/Max binding and decrease in histone acetylation at the telomerase reverse transcriptase promoter during differentiation of HL60 cells. Proc Natl Acad Sci, USA. 2001; 98:3826–31. [PubMed: 11274400]
17. Li M, Luo J, Brooks CL, Gu W. Acetylation of p53 inhibits its ubiquitination by Mdm2. J Biol Chem. 2002; 277:50607–11. [PubMed: 12421820]
18. Ouwehand K, de Ruijter A, van Bree C, Caron H, van Kuilenburg A. Histone deacetylase inhibitor BL1521 induces a G1-phase arrest in neuroblastoma cells through altered expression of cell cycle proteins. FEBS Lett. 2005; 579:1523–8. [PubMed: 15733867]

19. Oda K, Arakawa H, Tanaka T, et al. p53AIP1, a potential mediator of p53-dependent apoptosis, and its regulation by Ser-46-phosphorylated p53. Cell. 2000; 102:849–62. [PubMed: 11030628]
20. He L, Hannon GJ. MicroRNAs: Small RNAs with a big role in gene regulation. Nat Rev Genet. 2004; 5:522–31. [PubMed: 15211354]
21. Bartel DP. MicroRNAs: Target Recognition and regulatory functions. Cell. 2009; 136:215–33. [PubMed: 19167326]
22. Dai Y, Chen S, Venditti CA, et al. Vorinostat synergistically potentiates MK-0457 lethality in chronic myelogenous leukemia cells sensitive and resistant to imatinib mesylate. Blood. 2008; 112:793–804. [PubMed: 18505786]
23. Fiskus W, Wang Y, Joshi R, et al. Cotreatment with vorinostat enhances activity of MK-0457 (VX-680) against acute and chronic myelogenous leukemia cells. Clin Cancer Res. 2008; 14:6106–15. [PubMed: 18829489]
24. Ohyashiki JH, Sashida G, Tauchi T, Ohyashiki K. Telomeres and telomerase in hematologic neoplasia. Oncogene. 2002; 21:680–7. [PubMed: 11850796]
25. Harley CB. Telomerase and cancer therapeutics. Nature Rev Cancer. 2008; 8:167–79. [PubMed: 18256617]
26. Suenaga M, Soda H, Oka M, et al. Histone deacetylase inhibitors suppress telomerase reverse transcriptase mRNA expression in prostate cancer cells. Int J Cancer. 2002; 97:621–5. [PubMed: 11807787]
27. Woo HJ, Lee SJ, Choi BT, Park YM, Choi YH. Induction of apoptosis and inhibition of telomerase activity by trichostatin A, a histone deacetylase inhibitor, in human leukemic U937 cells. Exp Mol Pathol. 2007; 82:77–84. [PubMed: 16574101]
28. Hou M, Wang X, Popov N, et al. The histone deacetylase inhibitor trichostatin A derepresses the telomerase reverse transcriptase (hTERT) gene in human cells. Exp Cell Res. 2002; 274:25–34. [PubMed: 11855854]
29. Atkinson SP, Hoare SF, Glasspool RM, Keith WN. Lack of telomerase gene expression in alternative lengthening of telomere cells is associated with chromatin remodeling of the hTR and hTERT gene promoters. Cancer Res. 2005; 65:7585–90. [PubMed: 16140922]
30. Günes C, Lichtsteiner S, Vasserot AP, Englert C. Expression of the hTERT gene is regulated at the level of transcriptional initiation and repressed by Mad1. Cancer Res. 2000; 60:2116–21. [PubMed: 10786671]
31. Oh S, Song YH, Yim J, Kim TK. Identification of Mad as a repressor of the human telomerase (hTERT) gene. Oncogene. 2000; 19:1485–90. [PubMed: 10723141]
32. Ohyashiki K, Ohyashiki JH, Iwama H, Hayashi S, Shay JW, Toyama K. Telomerase activity and cytogenetic changes in chronic myeloid leukemia with disease progression. Leuk. 2007; 11:190–4.
33. Uziel O, Fenig E, Nordenberg J, et al. Imatinib mesylate (Gleevic) downregulates telomerase activity and inhibits proliferation in telomerase-expressing cell lines. Br J Cancer. 2005; 92:188–91. [PubMed: 15570306]
34. Yamada O, Kawauchi K, Akiyama M, Ozaki K, Motoji T, Adachi T, Aikawa E. Leukemic cells with increased telomerase activity exhibit resistance to imatinib. Leuk Lymphom. 2008; 49:1168–77.
35. Lu J, Getz G, Miska EA, et al. MicroRNA expression profiles classify human cancers. Nature. 2005; 435:834–8. [PubMed: 15944708]
36. Navarro A, Gaya A, Martinez A, et al. MicroRNA expression profiling in classic Hodgkin lymphoma. Blood. 2008; 111:2825–32. [PubMed: 18089852]
37. Woods K, Thompson JM, Hammond SM. Direct regulation of an oncogenic micro-RNA cluster by E2F transcription factors. J Biol Chem. 2007; 282:2130–4. [PubMed: 17135268]
38. Cimmino A, Calin GA, Fabbri M, et al. miR-15 and miR-16 induce apoptosis by targeting Bcl-2. Proc Natl Acad Sci USA. 2005; 102:13944–9. [PubMed: 16166262]
39. Xia L, Zhang D, Du R, et al. miR-15b and miR-16 modulate multidrug resistance by targeting Bcl-2 in human gastric cancer cells. Int J Cancer. 2008; 123:372–9. [PubMed: 18449891]
40. He L, He X, Lim LP, et al. A microRNA component of the p53 tumor suppressor network. Nature. 2007; 447:1130–4. [PubMed: 17554337]

41. Eis PS, Tam W, Sun L, et al. Accumulation of miR-155 and BIC RNA in human B cell lymphomas. Proc Natl Acad Sci USA. 2005; 102:3627–32. [PubMed: 15738415]

42. Kluiver J, Poppema S, de Jong D, et al. BIC and miR-155 are highly expressed in Hodgkin, primary mediastinal and diffuse large B cell lymphomas. J Pathol. 2005; 207:243–9. [PubMed: 16041695]

43. Levati L, Alvino E, Pagani E, et al. Altered expression of selected microRNAs in melanoma: antiproliferative and proapoptotic activity of miRNA-155. Int J Oncol. 2009; 35:393–400. [PubMed: 19578755]

44. Georgantas RW, Hildreth R, Morisot S, et al. CD34+ hematopoietic stem-progenitor cell microRNA expression and function: A circuit diagram of differentiation control. Proc Natl Acad Sci USA. 2007; 104:2750–5. [PubMed: 17293455]

45. Cheng YC, Lin H, Huang MJ, Chow JM, Lin S, Liu HE. Downregulation of c-Myc is critical for valproic acid-induced growth arrest and myeloid differentiation of acute myeloid leukemia. Leuk Res. 2007; 31:1403–11. [PubMed: 17445886]

46. Mann BS, Johnson JR, Cohen MH, Justice R, Pazdur R. FDA Approval Summary: Vorinostat for Treatment of Advanced Primary Cutaneous T-Cell Lymphoma. Oncologist. 2007; 12:1247–52. [PubMed: 17962618]

47. Li N, Zhao D, Kirschbaum M, et al. HDAC inhibitor reduces cytokine storm and facilitates induction of chimerism that reverses lupus in anti-CD3 conditioning regimen. Proc Natl Acad Sci USA. 2008; 105:4796–801. [PubMed: 18347343]

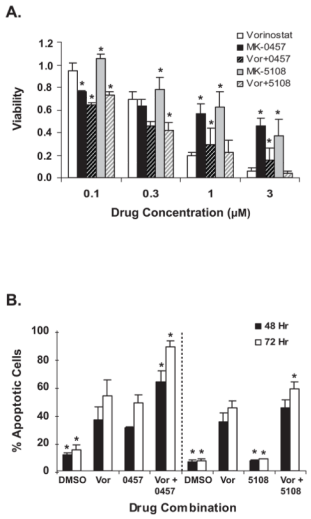

Figure 1.

Drug toxicity. **A.** L540 cell growth inhibition measured by MTS assay after 72 hours treatment with vorinostat (vor) or two different aurora kinase inhibitors, MK-0457 and MK-5108. **B.** Apoptotic response of L540 cells at 48 and 72 hours, measured by Annexin-V assay. Drug treatments from left to right: 1) DMSO = control for left half of graph; 2) Vor = 1.5 μM vorinostat for left half of graph; 3) 0457 = 0.1 μM MK-0457; 4) Vor + 0457 = 1.5 μM vor + 0.1 μM MK-0457; 5) DMSO = control for right half of graph; 6) Vor = 1.5 μM vor for right half of graph; 7) 5108 = 0.1 μM MK-5108; 8) Vor + 5108 = 1.5 μM vor + 0.1 μM MK-5108. Experiments with MK-0457 (left of dotted line) were done separately from those with MK-5108 (right of dotted line), thus average apoptotic values with DMSO (1 and 5) and vorinostat (2 and 6) vary within the range of their standard deviations.

In all graphs, data are average of three experiments and error bars represent standard deviation. Dunnet's t-test was used to compare all treatments to the corresponding vorinostat treatment (for panel B comparisons were made with vorinostat values on appropriate half of the graph). * = $p < 0.05$

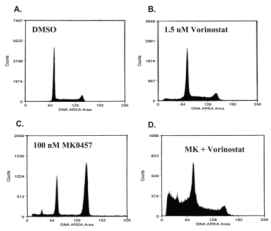

Figure 2.

Flow cytometry data for L540 cell cycle effects of vorinostat and the AKi MK-0457 after forty-eight hours of treatment, assayed for DNA content by propidium iodide. Cell cycle profiles are shown for cells treated with **A.** DMSO. **B.** 1.5 μM vorinostat. **C.** 0.1 μM MK-0457. **D.** both drugs. Percentages of cells in each cycle stage are in listed in Supplementary Table 1.

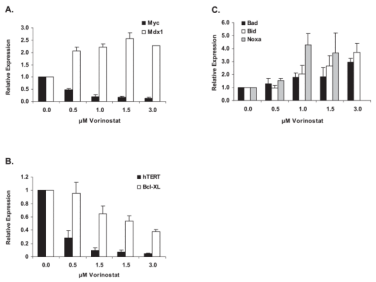

Figure 3.

L540 cell gene expression changes in response to vorinostat dose by real-time PCR. Regression analysis was performed to determine the relationship of vorinostat dose to the expression of each gene. The R-square represents the amount of variation between the model and the data. An R-square of 1 represents a perfect dose-response relationship. Panel **A.** Expression levels of c-Myc and its antagonist Mxd1 at four hours. For Myc R^2 = 0.68 and p = 0.013; for Mxd1 R^2 = 0.93 and p = 0.025. **B.** Expression levels of hTERT and Bcl-X_L at twenty-four hours. For hTERT R^2 = 0.40 and p = 0.018; for Bcl-X_L R^2 = 0.99 and p = 0.0012. **C.** Expression levels of Bad, Bid and Noxa at four hours. For Bad R^2 = 0.998 and p < 0.0001; for Bid R^2 = 0.987 and p = 0.0004; for Noxa R^2 = 0.94 and p = 0.015. Time points shown are those with maximal response; expression at other times shown in Supplemental Figure 2.

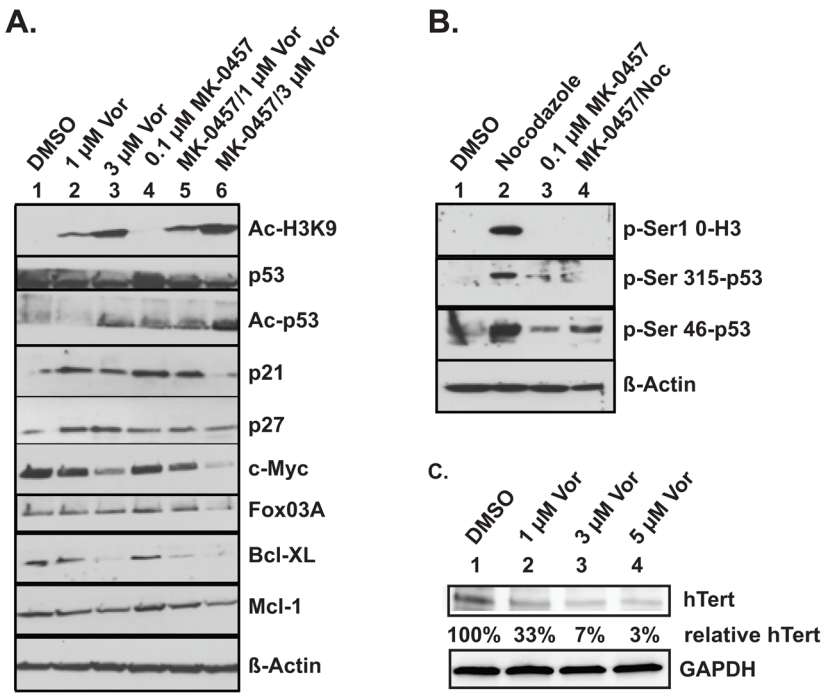

Figure 4.

Immunoblotting experiments. **A.** Protein confirmation of qPCR results and demonstration of acetylation changes in histone H3 and in p53. Results are from L540 cells treated twenty-four hours as indicated above each lane. **B.** Phosphorylation levels of indicated amino acid residues in histone H3 and in p53, in freely cycling cells (DMSO) versus cells enriched in the G2/M phase by twenty (nocodazole) or twenty-four (MK-0457) hours of treatment with the drugs indicated above each lane. **C.** Western blot analysis reveals decreased hTERT protein levels after treatment with vorinostat in a dose-dependent manner. % hTert levels shown are normalized to GAPDH levels and relative to the DMSO control. Vor = vorinostat, Noc = 40 ng/ml Nocodazole, MK-0457 = 0.1 μM MK-0457

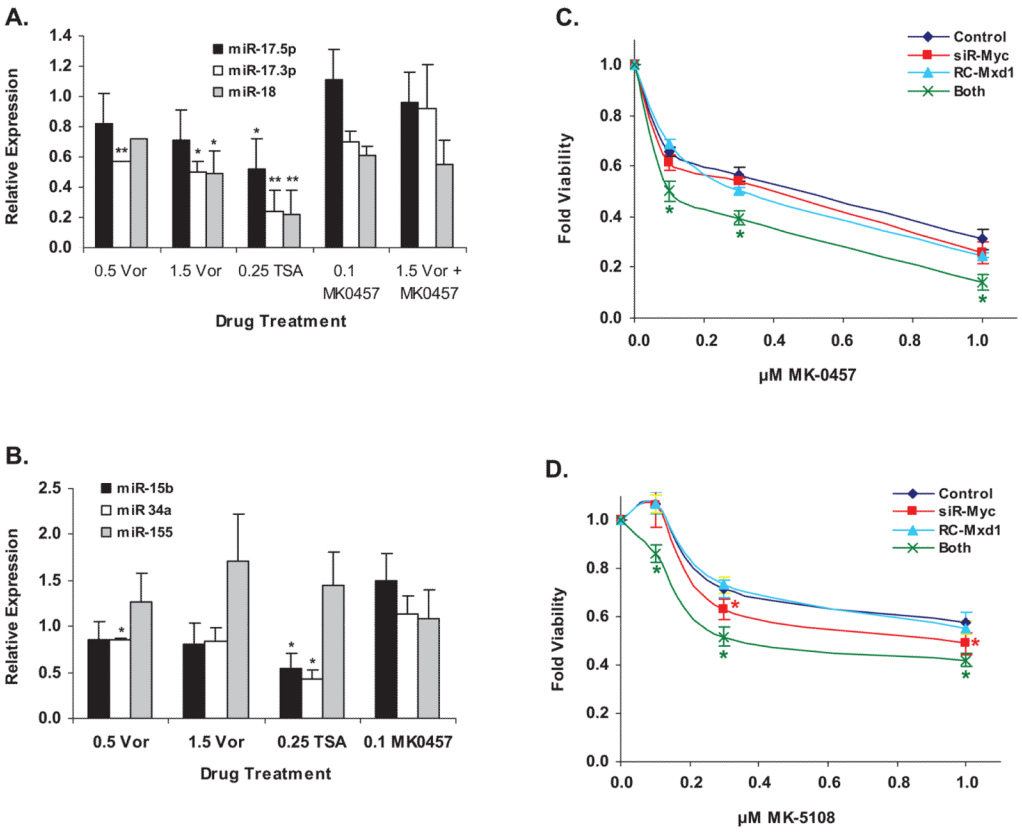

Figure 5.

Importance of c-myc levels. **A.** and **B:** Changes in miRNA expression levels in L540 lymphoma cells in response to drug treatment; concentrations of drugs listed are in µM. Vor = vorinostat; TSA = trichostatin-A. Paired t-test was used to compare if the fold change in relative expression of a gene under a specific treatment was significantly different from DMSO control. **A.** Changes in Myc-regulated miRNAs in L540 cells. **B.** Changes in non-myc-regulated miRNAs in L540 cells. **C.** Effect of myc knock-down and/or Mxd1 over-expression on sensitivity of L540 cells to MK-0457. **D.** Same as panel C for MK-5108 sensitivity. For panels C and D, Dunnett's t-test was used to compare differences between the control and other treatments at each dose level.

Table 1

IC_{50} values in μM for the lymphoma cell lines listed on the left. Numbers in parentheses (N) are the number of separate experiments used to determine each IC_{50} value. The combination index (CI) for each AKi + vorinostat in the cell lines listed. The values for (N) represent the number of separate experiments used to determine each CI value.

	IC_{50} values in μM +/− standard deviation (N)			Combination Indices +/− standard deviation (N)	
Cell Type	**Vorinostat**	**MK-0457**	**MK-5108**	**Vor + MK-0457**	**Vor +MK-5108**
L540	**0.58** +/− 0.10 (5)	**0.66** +/−0.09 (4)	**1.51** +/− 0.21 (4)	**0.44** +/− 0.150 (4)	**0.59** +/− 0.076 (3)
KM-H2	**0.51** +/− 0.05 (6)	**0.34** +/−0.10 (3)	**2.77** +/− 0.39 (4)	**0.66** +/− 0.032 (2)	**0.50** +/− 0.043 (3)
Daudi	**0.41** +/− 0.10 (6)	**0.06** +/− 0.0 (6)	**0.23** +/− 0.03 (2)	**1.15** (1)	**1.14** +/− 1.060 (2)
DHL-4	**0.63** +/− 0.09 (4)	**0.20** +/− 0.03 (3)	**0.33** +/− 0.09 (4)	**1.00** +/− 0.991 (2)	**0.93** +/− 0.144 (2)
DHL-6	**0.47** +/− 0.18 (3)	**4.5** +/− 0.71 (2)	**0.51** +/− 0.13 (3)	**0.74** (1)	**0.56** +/− 0.055 (2)
L1236	**0.60** +/− 0.08 (5)	N.D.	N.D.	**0.36** +/− 0.003 (2)	**0.69** +/− 0.078 (3)
U937	**1.50** +/− 0.14 (4)	**0.44** +/− 0.16 (3)	**1.27** +/− 0.42 (3)	**0.65** +/− 0.144 (2)	**0.85** (1)